

## Self-Driven Synchronous Rectifier for DC Motor Driver with Parasitic Capacitor Based ZVS

**Burli Lakshmana Rao**

M.Tech Student

Department of Electrical & Electronics Engineering,  
Thandra Paparaya Institute of Science & Technology,  
Bobbili; Vizianagaram (Dt);  
A.P, India.

**B.Venkata Ramana**

Assistant Professor & HoD

Department of Electrical & Electronics Engineering,  
Thandra Paparaya Institute of Science & Technology,  
Bobbili; Vizianagaram (Dt);  
A.P, India.

### Abstract

*The single-phase self-driven synchronous rectification (SDSR) technique to multiphase ac-dc systems. Power MOSFETs with either voltage- or current-sensing self-driven gate drives are used to replace the diodes in the rectifier circuits. The generalized methodology allows multiphase SDSRs to be designed to replace the multiphase diode rectifiers. Unlike the traditional SR that is designed for high-frequency power converters, the SDSR proposed here can be a direct replacement of the power diode bridges for both low- and high-frequency operations. The SDSR utilizes its output dc voltage to supply power to its control circuit. No start-up control is needed because the body diodes of the power MOSFETs provide the diode rectifier for the initial start-up stage. The generalized method is demonstrated in 2-kW one-phase and three-phase SDSRs for inductive, capacitive, and resistive loads. Power loss reduction in the range of 50%-69% has been achieved for the resistive load. In this project, a soft-switching buck power-factor-correction (PFC) converter for a high-efficiency AC-DC light-emitting diode (LED) driver is proposed. By replacing a freewheeling diode with a self-driven synchronous rectifier (SR), efficiency improvement is achieved due to the reduced conduction loss on the SR. In addition, there is no switching loss on switching devices because zero-voltage-switching (ZVS) operations of both switches are easily performed. Since the SR is self-driven without an additional control circuit, the proposed converter has competitive price. In order to verify efficiency improvement of the proposed converter, it is compared with a conventional critical-*

*conduction-mode (CRM) buck PFC converter. The efficiency of the proposed converter is measured maximum 95.61% at 170 [Vac] and improved maximum 0.23% at 240 [Vac]. For verifying soft-switching and efficiency improvement of the proposed converter, design consideration by using MATLAB/Simulink.*

*Index Terms*—Buck-boost converter, LED driver, power factor correction (PFC), synchronous rectifier, zero-voltage-switching (ZVS).

### I. INTRODUCTION

Electric Lighting is an essential part of our lives, and is a major component in energy consumption. The types of lighting devices commonly adopted for electric lighting is the incandescent lamps, the gas-discharge lamps and solid state lighting devices. There are various dimming techniques introduced for different types of lighting devices. For incandescent lamps, dimming is typically performed by controlling the firing angle of a thyristor.

For Gas discharge lamps, dimming technique revolve around the control of voltage level, duty cycle and frequency. For solid-state lighting devices, the dimming technique is to vary the dc level of the forward current [1].

The high efficiency LED system needs the high-efficiency power supply to feed the LED [2]. LEDs are very attractive lighting sources due to their excellent characteristics. Many types of power switching converter used to adapt primary energy sources to the

requirements [3]. HB LEDs have been widely accepted because of superior longevity, Low-maintenance requirements and improve luminance. For an LED load, a small variation in driving voltage leads to large variation in the LED current. LED current with large ripple will lead to seriously affect the reliability and longevity [4].

On the other hand, a buck PFC converter and a buck-boost PFC converter have high efficiency owing to the simple structure and low output voltage in a LED driver [5]–[6]. These converters are usually operated in the discontinuous conduction mode (DCM) and critical conduction mode (CRM). Among them, CRM control is highly preferred because its turn-on switching loss and the diode reverse-recovery loss are almost eliminated. In addition, the input filter design is easier than the DCM operation [7]–[10]. Nevertheless, conduction loss of the diode still exists, and it decreases the power conversion efficiency. For this reason, a synchronous rectifier (SR) is proposed to be used instead of a diode. The synchronous rectification controller proposed in uses an auxiliary winding of the transformer for detecting voltage and current. In a Smart Rectifier control IC and a dual-mode SR controller were used for driving the SR.

## II. ANALYSIS OF PROPOSED CONVERTER

The circuit diagram of the proposed AC-DC converter is shown in Fig.1. The EMI input filter includes a filter inductor  $L_f$  and a filter capacitor  $C_f$ . The main structure of the proposed AC-DC converter is similar to that of a conventional buck-boost converter, which consists of an input capacitor  $C_{in}$ , an output capacitor  $C_o$ , a buck-boost inductor  $L_b$ , and a main switch  $S_m$ , the only difference being that the output diode is replaced with SR  $S_a$ . Diodes  $D_{sm}$  and  $D_{sa}$  are the intrinsic body diodes of  $S_m$  and  $S_a$ , respectively. Capacitors  $C_{sm}$  and  $C_{sa}$  denote the parasitic output capacitances of  $S_m$  and  $S_a$ , respectively. For the analysis of the proposed AC-DC converter in a steady state, several assumptions are made during one switching period  $T_s$ . All the semiconductor devices are ideal components except

for the output capacitances  $C_{sm}$  and  $C_{sa}$  of  $S_m$  and  $S_a$ , respectively.

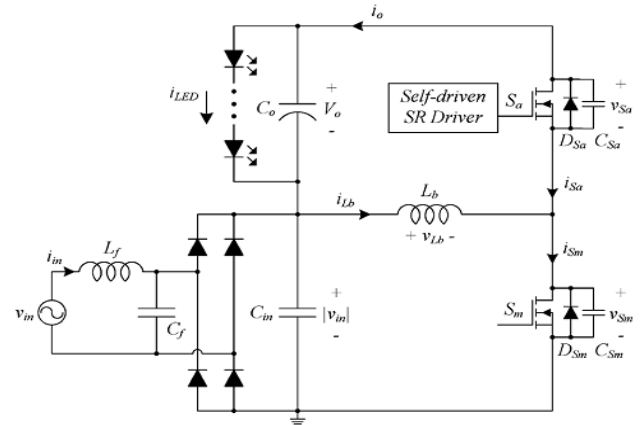


Fig.1. Proposed AC-DC converter with a self-driven synchronous rectifier.

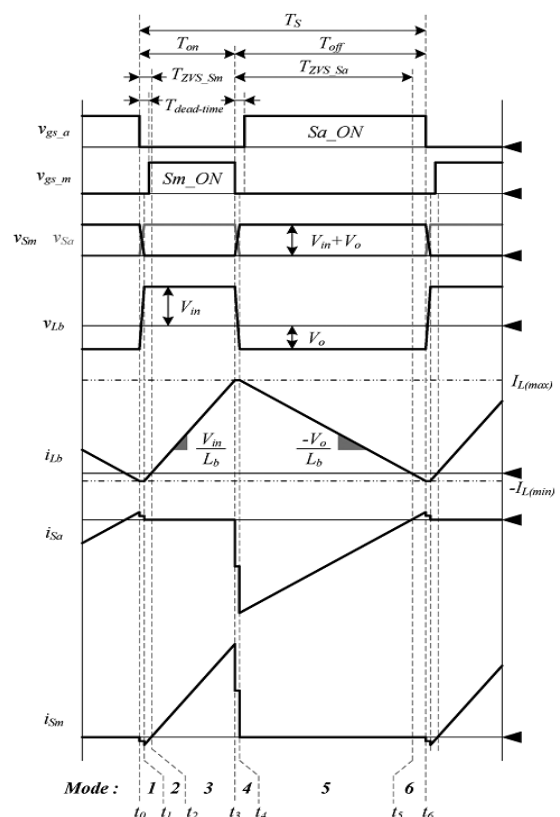


Fig. 2. Theoretical waveforms of proposed converter.

The capacitance of the output capacitor,  $C_o$ , is large enough to consider the output voltage  $V_o$  as a constant. The rectified line voltage  $|v_{1R}|$  is considered as a constant value  $V_{in}$  during a switching period because



charging, and  $C_{sa}$  begins discharging. By assuming that the capacitances of the parasitic output capacitors,  $C_{sm}$  and  $C_{sa}$ , are very small and the time interval between  $t_3$  and  $t_4$  is very short, the inductor current  $i_{Lb}$  is regarded as a constant value  $I_{L(max)}$ . Voltages  $V_{sm}$  and  $V_{sa}$  vary linearly. The transition time interval  $T_{t2}$  is expressed as follows:

$$T_{t2} = (C_{Sm} + C_{Sa}) \frac{V_{in} + V_o}{I_{L(max)}} \quad (4)$$

**Mode 5 [ $t_4, t_5$ ]:** At  $t_4$ , capacitor  $C_{sa}$  is fully discharged, and voltage  $V_{sa}$  reaches zero when  $D_{sa}$  is turned on. ZVS operation of  $S_a$  is performed because the switch voltage  $V_{sa}$  is zero even before the gate pulse of  $S_a$  is applied. Furthermore, gate pulse  $V_{gs_a}$  is applied to the gate to turn switches  $S_a$  on. As the inductor voltage  $V_{Lb}$  is  $-V_o$ , the inductor current  $I_{Lb}$  decreases linearly as follows

$$i_{Lb}(t) = I_{L(max)} - \frac{V_o}{L_b}(t - t_4) \quad (5)$$

**Mode 6 [ $t_5, t_6$ ]:** This mode begins when the inductor current  $I_{Lb}$  changes direction from positive to negative. Voltage  $V_{Lb}$  is equal to  $-V_o$ , and current  $i_{Lb}$  decreases linearly with the slope of  $V_o/L_b$ . At the end of this mode, current  $i_{Lb}$  reaches its minimum value  $-I_{L(min)}$ , where  $T_{off}$  is the time interval between  $t_4$  and  $t_6$ . Time  $T_{t2}$  is very short; therefore, it is not considered.

$$-I_{L(min)} = I_{L(max)} - \frac{V_o}{L_b} T_{off}, \quad (6)$$

### III. ANALYSIS OF SELF-DRIVEN SR CIRCUIT

The circuit diagram of the proposed self-driven SR driver is shown in Fig.4. The SR driver is composed of three resistors:  $R_1$ ,  $R_2$  and  $R_3$ ; diodes:  $D_1$  and  $D_2$ ; capacitors:  $C_1$  and  $C_2$ ; a transistor  $Q_1$ ; and a MIC4427 MOSFET driver. The auxiliary control power is bootstrapped from the main control power  $+V_{cc}$ . Diode  $D_2$  is used as a bootstrap diode. Diode  $D_1$  is employed to detect the polarity of the switch voltage  $V_{sa}$ . Resistors  $R_2$  and  $R_3$  transistor  $Q_1$  are used to obtain high and low signals according to the polarity of  $V_{sa}$ . Furthermore, the collector emitter voltage  $V_{ce}$  is applied to MIC4427 for driving the SR.

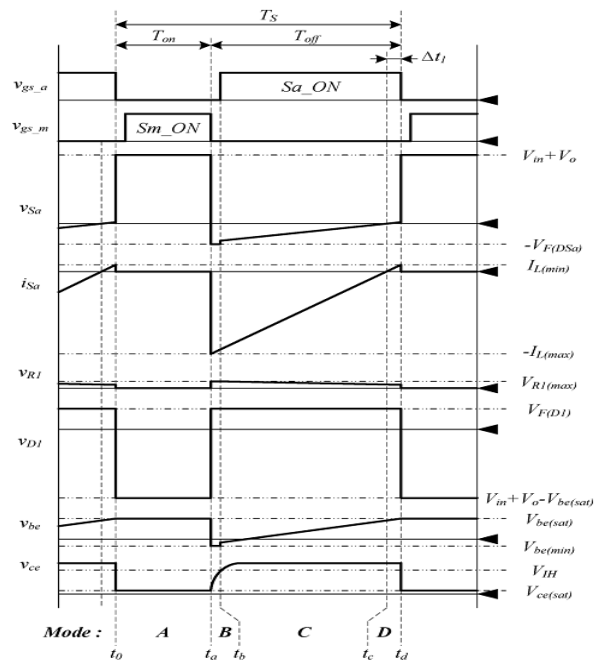


Fig.5. Theoretical waveforms of proposed SR driver.

For generating the dead time in the proper ZVS operation of  $S_a$ , a small capacitance  $C_1$  is added to the SR driver. In addition, a small resistance  $R_1$  is added to compensate for the difference in the forward voltage drop  $V_{F(D1)}$  and the base-emitter saturation voltage  $V_{be(sat)}$ . The basic operation of the SR driver is as follows. When voltage  $V_{sa}$  is negative, diode  $D_1$  conducts and the base-emitter voltage  $V_{be}$  becomes lower than  $V_{be(sat)}$ . Thus, the turn-on gate pulse from MIC4427 is applied to  $S_a$ . For the analysis of the proposed SR driver in a steady state, several assumptions are made during one switching period  $T_s$ . Capacitor  $C_2$  is large enough to consider the control power  $V_{aux}$  as a constant. Diode  $D_1$  is an ideal component. Transistor  $Q_1$  acts as a switching device, not as a signal amplifier. In addition, the base-emitter input capacitor and collect-emitter output capacitor are not considered. Switch  $S_a$  is an ideal component, except for the drain-source on-resistance  $R_{DS(on)}$ . The theoretical waveforms of the proposed SR driver in a switching period  $T_s$  are shown in Fig.5. All the operating modes of the proposed SR driver are shown in Fig.6. Before  $t_0$ , switch  $S_a$  is turned on, and diode  $D_1$  conducts. The base-emitter voltage  $V_{be}$  increases



$$i_{R2}(t_d) = \frac{V_{aux} - V_{be(sat)}}{R_2}, \quad (14)$$

$$i_{Sa}(t_d) = \frac{V_o}{L_b} \Delta t_1, \quad (15)$$

Where is the time interval between and . By substituting (14) and (15) into (13), the time interval is expressed as

$$\Delta t_1 = \left( \frac{R_1 + R_2}{R_2} V_{be(sat)} - V_{F(D1)} - \frac{R_1}{R_2} V_{aux} \right) \times \frac{L_b}{V_o \cdot R_{DS(on)}}. \quad (16)$$

Therefore, the time interval, which is related to the ZVS operation, is easily controlled by adjusting resistance .In the proposed converter, the ZVS conditions for and are expressed as

$$T_{dead-time} < T_{ZVS\_Sm}, \quad (17)$$

$$T_{dead-time} < T_{ZVS\_Sa}, \quad (18)$$

Where is the dead time of switches and for a proper ZVS operation, and are the times when each switch is reverse-biased and the reverse current flows through the intrinsic body diode of each switch. The gate pulse should be applied to each switch after voltage or has decreased to zero and before the current flowing though the intrinsic body diode changes its direction. Thus, the dead time should be considered. The ZVS operation of is always satisfactory because is sufficiently longer than. By assuming that the time interval between and

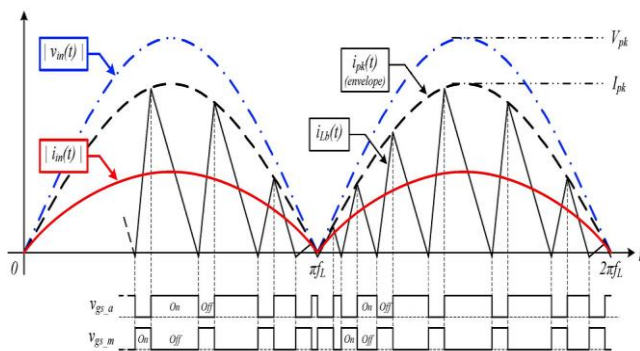


Fig.7. Theoretical Waveforms of Rectified Input Line Voltage, Input Current, and Inductor Current in a Line Period.

## IV.DC MOTORS

Almost every mechanical movement that we see around us is accomplished by an electric motor. Electric machines are a means of converting energy. Motors take electrical energy and produce mechanical energy. Electric motors are used to power hundreds of devices we use in everyday life. Motors come in various sizes. Huge motors that can take loads of 1000’s of Horsepower are typically used in the industry. Some examples of large motor applications include elevators, electric trains, hoists, and heavy metal rolling mills. Examples of small motor applications include motors used in automobiles, robots, hand power tools and food blenders. Micro-machines are electric machines with parts the size of red blood cells, and find many applications in medicine.

Electric motors are broadly classified into two different categories: DC (Direct Current) and AC (Alternating Current). Within these categories are numerous types, each offering unique abilities that suit them well for specific applications. In most cases, regardless of type, electric motors consist of a stator (stationary field) and a rotor (the rotating field or armature) and operate through the interaction of magnetic flux and electric current to produce rotational speed and torque. DC motors are distinguished by their ability to operate from direct current. There are different kinds of D.C. motors, but they all work on the same principles. In this chapter, we will study their basic principle of operation and their characteristics. It’s important to understand motor characteristics so we can choose the right one for our application requirement.

## V.MATLAB/SIMULATION RESULTS

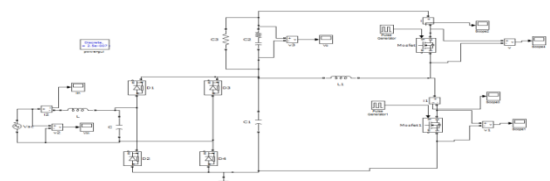


Fig.8. Matlab/Simulation Model of Proposed AC-DC Converter with a Self-Driven Synchronous Rectifier.

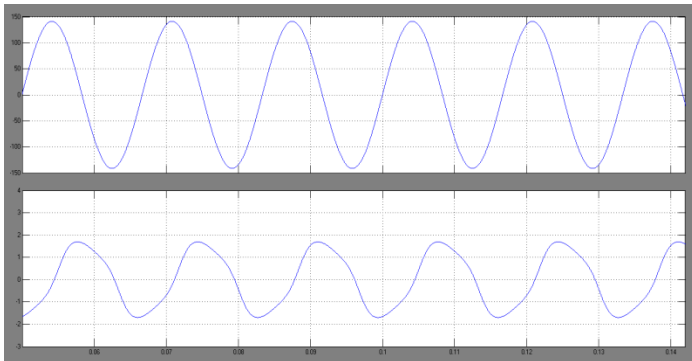


Fig.9.Simulation Waveforms At  $V_{in}=100$ , Input Voltage ( $V_{in}$ ) And Current ( $I_{in}$ ).

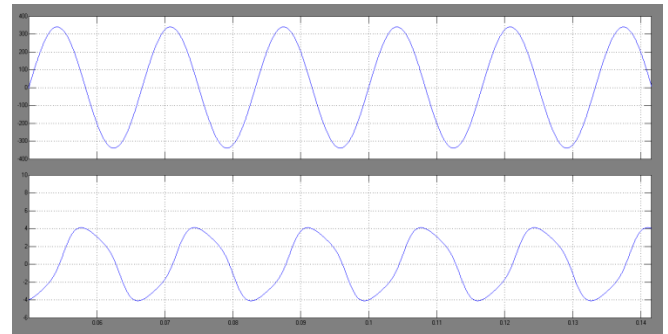


Fig.13.Simulation Waveforms at  $V_{in}=240$ , Input Voltage ( $V_{in}$ ) and Current ( $I_{in}$ ).

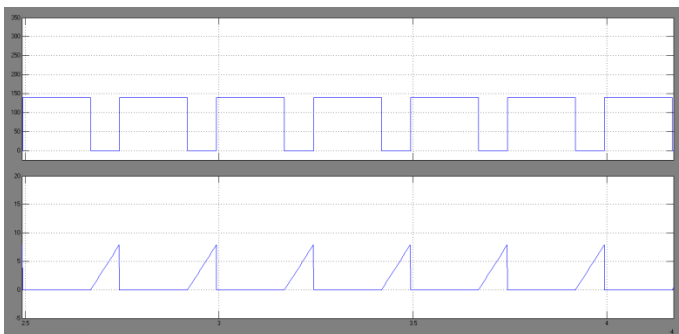


Fig.10.Switch Voltage ( $V_{gsm}$ ) And Current( $I_{gsm}$ ).

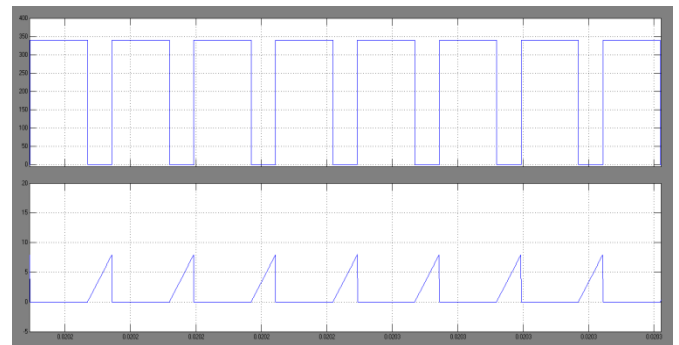


Fig.14.Switch Voltage ( $V_{gsm}$ ) and Current( $I_{gsm}$ ).

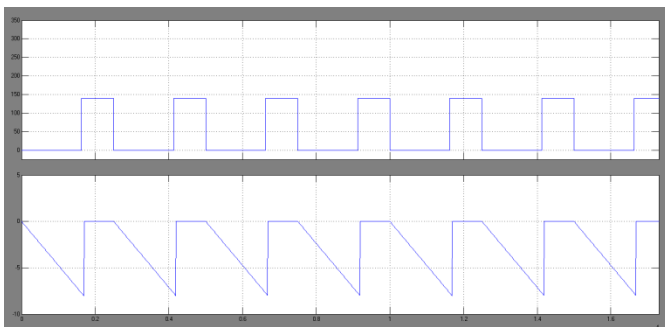


Fig.11.Switch Voltage ( $V_{gs\_a}$ ) and Current ( $I_{gsa}$ ).

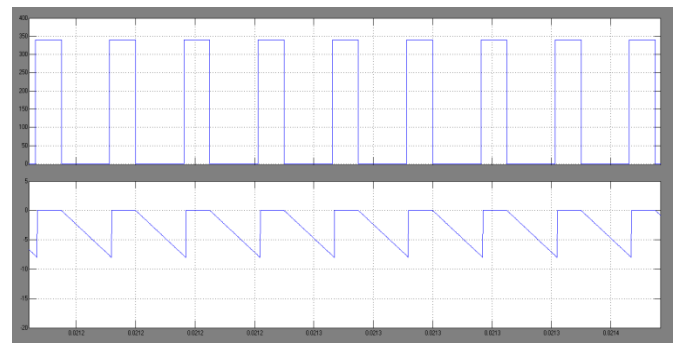


Fig.15.Switch Voltage ( $V_{gs\_a}$ ) and Current ( $I_{gsa}$ ).

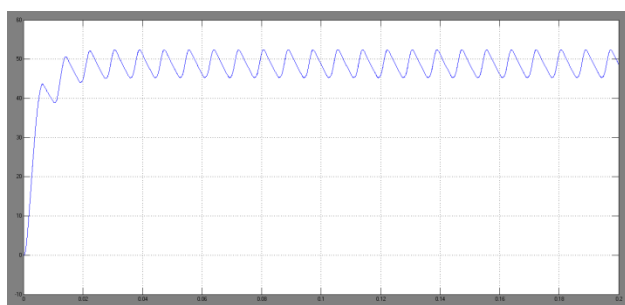


Fig.12.Output Voltage.

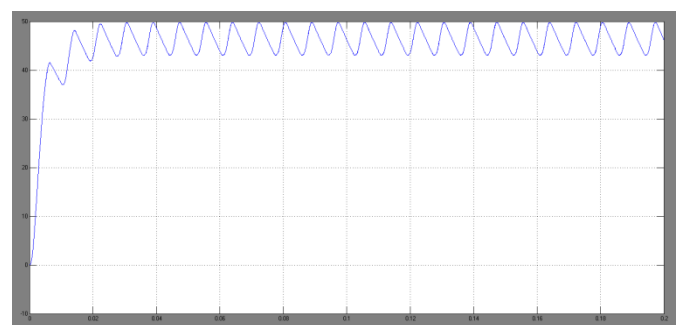
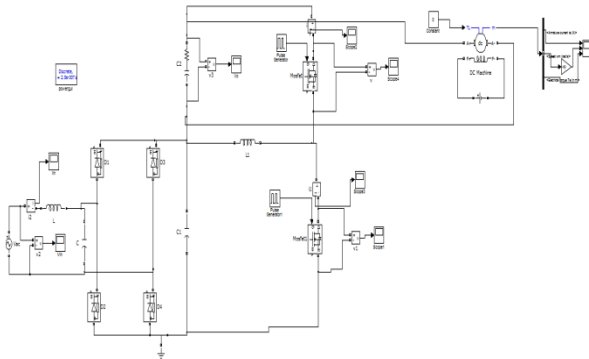
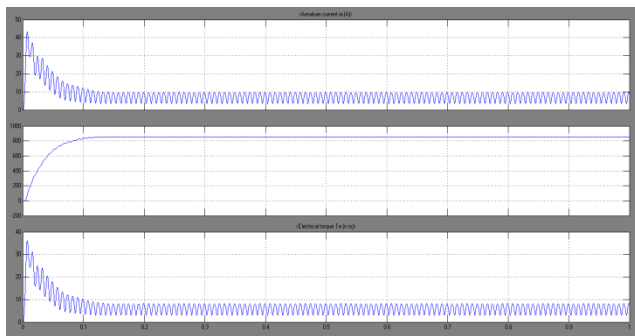


Fig.16.Output Voltage.



**Fig.17. Matlab/Simulation Model of Proposed AC-DC Converter with a self-driven Synchronous Rectifier with DC Motor.**



**Fig.18. Simulation Wave Forms of Current, Speed and Torque.**

## VI. CONCLUSION

In this paper, a ZVS AC-DC LED driver using a self-driven SR has been proposed. In the proposed converter, ZVS operation of both and is performed. In addition, by using a self-driven SR driver, the conduction loss of the output rectifier is significantly reduced, and high efficiency is achieved. Moreover, the power factor is also improved by means of the time interval. The Proposed AC-DC Converter with a self-driven Synchronous Rectifier with DC Motor. DC motor application based on this paper we can performer the speed-torque characteristics.

## REFERENCES

[1] M. Arias, D. G. Lamar, F. F. Linera, D. Balocco, A. A. Diallo, and J. Sebastian, "Design of a soft-switching asymmetrical half-bridge con verter as second stage of an LED driver for street lighting

application," *IEEE Trans. Power Electron.*, vol. 27, no. 3, pp. 1608–1621, Mar. 2012.

[2] S. Saponara, G. Pasetti, N. Costantino, F. Tinfena, P. D. Abramo, and L. Fanucci, "A flexible LED driver for automotive lighting appli cations: IC design and experimental characterization," *IEEE Trans. Power Electron.*, vol. 27, no. 3, pp. 1071–1075, Mar. 2012.

[3] Y.-T. Hsieh, B.-D. Liu, J.-F. Wu, C.-L. Fang, H.-H. Tsai, and Y.-Z. Juang, "A high-dimming-ratio LED driver for LCD backlights," *IEEE Trans. Power Electron.*, vol. 27, no. 11, pp. 4562–4570, Nov. 2012.

[4] S.-J. Choi and T.-H. Kim, "Symmetric current-balancing circuit for LED backlight with dimming," *IEEE Trans. Ind. Electron.*, vol. 59, no. 4, pp. 1698–1707, Apr. 2012.

[5] J. Cardesin, J. Ribas, J. G.-Garcia, M. R.-Secades, A. J. Calleja, E. L. Corominas, and M. A. D. Costa, "LED permanent emergency lighting system based on a single magnetic component," *IEEE Trans. Power Electron.*, vol. 24, no. 5, pp. 1409–1416, May 2009.

[6] S. Y. Hui, S. N. Li, X. H. Tao, W. Chen, and W. M. Ng, "A novel pas sive offline LED driver with long lifetime," *IEEE Trans. Power Elec tron.*, vol. 25, no. 10, pp. 2665–2672, Oct. 2010.

[7] Y.-C. Li and C.-L. Chen, "A novel primary-side regulation scheme for single-stage high-power-factor AC-DC LED driving circuit," *IEEE Trans. Ind. Electron.*, vol. 60, no. 11, pp. 4978–4986, Nov. 2013.

[8] C. Zhao, X. Xie, and S. Liu, "Multioutput LED drivers with precise passive current balancing," *IEEE Trans. Power Electron.*, vol. 28, no. 3, pp. 1438–1448, Mar. 2013.

[9] H.-L. Cheng, Y.-C. Hsieh, and C.-S. Lin, "A novel single-stage high power-factor AC/DC converter featuring high circuit efficiency," *IEEE Trans. Ind. Electron.*, vol. 58, no. 2, pp. 524–532, Feb. 2011.

[10] Y.-T. Huang, Y.-T. Chen, Y.-H. Liu, H.-C. Hsiao, and W.-T. Tsai, "Compact-size and high-conversion-efficiency regulator for alter nating-current-operated light-emitting diodes," *IEEE Trans. Ind. Electron.*, vol. 58, no. 9, pp. 4130–4135, Sep. 2011.

[11] D. G. Lamar, M. Arias, A. Rodriguez, A. Fernandez, M. M. Her nando, and J. Sebastian, "Design-oriented analysis and performance evaluation of a low-cost high-brightness LED driver based on flyback power factor corrector," *IEEE Trans. Ind. Electron.*, vol. 60, no. 7, pp. 2614–2626, Jul. 2013.

[12] S.-C. Moon, G.-B. Koo, and G.-W. Moon, "A new control method of interleaved single-stage flyback AC-DC converter for outdoor LED lighting systems," *IEEE Trans. Power Electron.*, vol. 28, no. 8, pp. 4051–4062, Aug. 2013.

[13] X. Xie, J. Wang, C. Zhao, Q. Lu, and S. Liu, "A novel output current estimation and regulation circuit for primary side controlled high power factor single-stage flyback LED driver," *IEEE Trans. Power Electron.*, vol. 27, no. 11, pp. 4602–4612, Nov. 2012.

[14] H.-H. Chou, Y.-S. Hwang, and J.-J. Chen, "An adaptive output current estimation circuit for a primary-side controlled LED driver," *IEEE Trans. Power Electron.*, vol. 28, no. 10, pp. 4811–4819, Oct. 2013.

[15] X. Xie, C. Zhao, L. Zheng, and S. Liu, "An improved buck PFC converter with high power factor," *IEEE Trans. Power Electron.*, vol. 28, no. 5, pp. 2277–2284, May 2013.